Letter | Editors' Suggestion

Beyond Tate's law: Geometric control of pendant drop detachment

Bauyrzhan K. Primkulov*
Yale University, New Haven, Connecticut, USA

(Received 29 January 2026; accepted 10 April 2026; published 11 May 2026)

The size of a pendant drop detaching from a capillary is classically set by the balance between gravity and surface tension, as described by Tate's law, implying only a weak dependence on nozzle size. I show that purely geometric confinement provides a simple and robust means to tune the detachment volume well below this classical limit. By placing a capillary between two superhydrophobic plates forming a shallow wedge, I demonstrate experimentally that drops detach at significantly reduced volumes. A scaling argument reveals that the wedge induces a capillary pressure gradient that assists gravity, yielding a simple relation between drop volume and confinement geometry that collapses all measurements. For completeness, I also consider the complementary case of drops resting on an inclined superhydrophobic surface, which enables volumes above the classical limit through a similarly simple geometric control.

DOI: 10.1103/95pk-yfpr

Drop generation is ubiquitous in both natural and engineered systems, ranging from breaking waves and waterfalls to inkjet printing [1] and microfluidic devices [2,3]. A particularly simple and widespread method for producing single drops of reproducible size occurs in clinical practice, where a deformable eyedrop bottle is squeezed to dispense a single drop. Despite substantial variability in the applied forcing, different users consistently generate nearly identical drops, highlighting a robust and passive mechanism of drop-size selection that requires no sophisticated equipment.

A drop suspended from the tip of a capillary tube detaches when its weight exceeds the surface-tension force pulling it toward the capillary. The balance of these forces at the time of detachment is widely known as Tate's law [4], $\rho g \Omega_0 \approx 2\pi a \gamma$, where ρ, Ω_0, and g are the liquid drop density, volume, and gravitational acceleration, and a and γ are the radius of the capillary tube and the surface tension, respectively. Tate's law can be rearranged to link the detached drop's natural size R_0 to the capillary length $\ell_c = \sqrt{\gamma/\rho g}$ and a through

$$R_0^3 \approx \tfrac{3}{2} a \ell_c^2. \tag{1}$$

Equation (1) highlights that the detached drop radius R_0 depends only weakly on the size of the tip a. For example, reducing R_0 by a factor of 2 would require reducing a by a factor of 8. Therefore, in practice the size of the detached drop is more readily tuned by altering ℓ_c than by changing the nozzle size.

An analogous problem arises in the detachment of gas bubbles from submerged orifices, where buoyancy replaces gravity as the driving force. In that case, the classical Fritz radius [5] provides the corresponding scaling for the bubble size at detachment [6,7]. This correspondence underscores the generality of the force balance governing drop and bubble detachment, and suggests that

*Contact author: bauyrzhan.primkulov@yale.edu

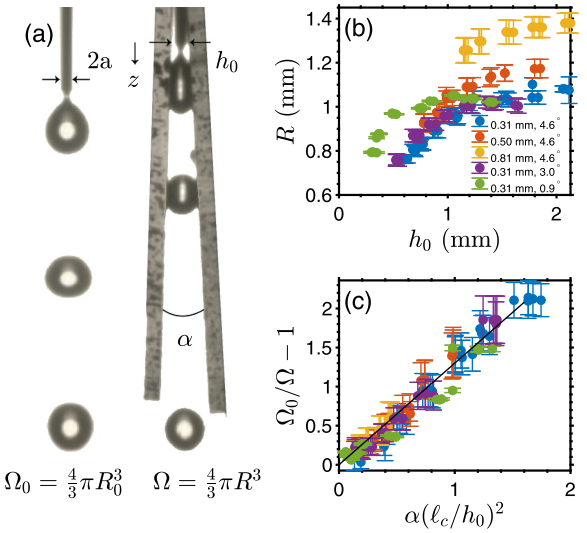

FIG. 1. (a) Squeezing a drop between two superhydrophobic plates induces early detachment of the pendant drop. (b) The size of the pendant drop depends weakly on the nozzle diameter $2a$, but can be strongly tuned by adjusting the distance h_0 and angle α between the plates. The legend indicates the values of $2a$ and α used in each experiment. (c) Scaling the drop volume data using Eq. (2) collapses the data from panel (b). The solid line corresponds to $c = 1.3$ in Eq. (2).

mechanisms that modify this balance—such as geometric confinement—may apply broadly across both systems. Here, I focus on the case of a pendant drop.

Some common strategies for triggering the earlier detachment of a drop include reducing surface tension near the tube tip via laser actuation [8], applying an electric field [9], or sending pressure pulses through the liquid [1]. These methods rely on external actuation or dynamic forcing.

In this manuscript, I explore the role that purely geometric confinement can play in triggering earlier detachment of pendant drops. I show that confinement alone can assist gravity at detachment, and I develop a simple scaling argument to rationalize the relation between the confinement geometry and the size of the detached pendant drop.

By placing a capillary between two superhydrophobic plates forming a shallow wedge [Fig. 1(a)], I impose a capillary pressure gradient that acts along the drop. Superhydrophobic plates were fabricated by coating glass slides with NeverWet spray. Slides were cleaned [soap, deionized (DI) water, isopropyl alcohol (IPA)], coated with NeverWet (base layer + four top layers), and cured for 12 hours to ensure robustness to mechanical wear (see Supplemental Material [10]). Experiments were performed with the same plates without observable degradation. Reported low-contact angle hysteresis for NeverWet surfaces ($7^\circ \pm 4^\circ$) [11] is consistent with my measurements (Fig. S1 [10]). All experiments were conducted by slowly feeding tap water through the capillary with a syringe pump. Detachment was captured with a Chronos 2.1-HD high-speed camera, and images were analyzed to recover the drop's projected area. In Fig. 1, R is inferred from the projected area assuming a spherical drop shape, while in Fig. 2 it is obtained from the volume of revolution of the detected interface. In both cases, the dominant uncertainty in the unperturbed radius R arose from inertia-capillary oscillations following detachment, and the uncertainty was taken as the frame-to-frame standard deviation of R (see Supplemental Material [10]). For velocity measurements (Fig. 3), drop centroid trajectories are fitted to quadratic functions of time. Residuals provide a positional uncertainty σ_{res}, propagated to $\delta u \sim \frac{1}{2}\sigma_{\text{res}}|d^2x/dt^2|$. Pendant-drop experiments were repeated by systematically varying the tube's outer diameter $2a \in [0.31, 0.50, 0.81]$ mm, the wedge angle $\alpha \in [0.9^\circ, 3.0^\circ, 4.6^\circ]$, and the spacing between the plates h_0, measured near the outlet

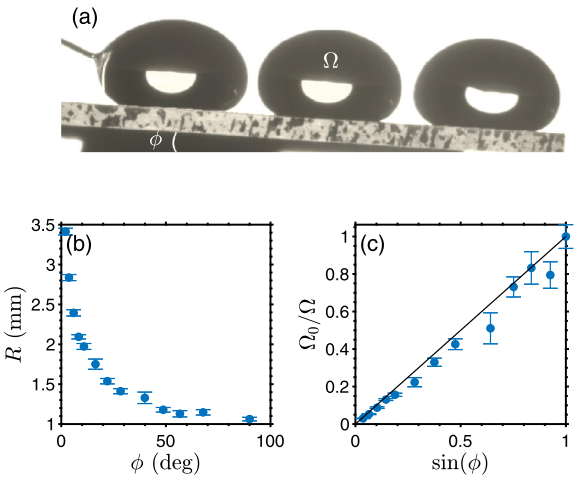

FIG. 2. (a) One can readily increase the drop volume above $\Omega_0 = \frac{4}{3}\pi R_0^3$ [see Fig. 1(a)] by resting the drop on a superhydrophobic surface inclined at an angle ϕ. (b) Larger drops are obtained at smaller ϕ, (c) consistent with the simple scaling given by Eq. (3).

of the capillary tube [see Fig. 1(a)]. All three parameters provide independent control over R, with experimental measurements summarized in Fig. 1(b): reducing h_0 always reduces R (given $\alpha > 0$), and this reduction is more effective at larger α, while a sets the drop radius limit at $h_0 \to \ell_c$.

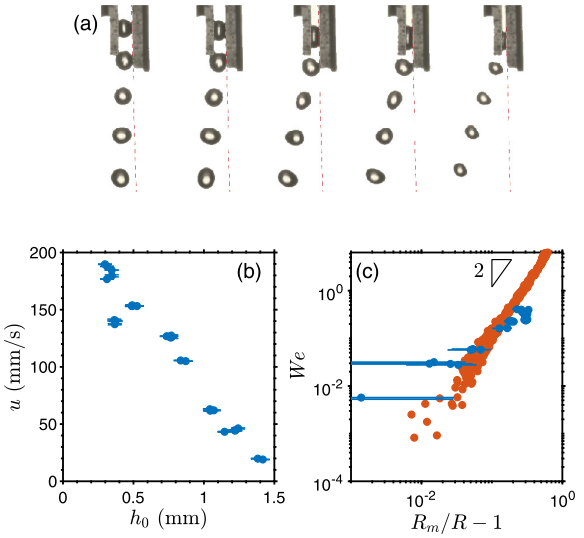

FIG. 3. (a) An offset between the superhydrophobic plates breaks symmetry and propels the drop horizontally. The red dashed line traces one of the plates. (b) Reducing the plate spacing increases the horizontal velocity. Data correspond to $h_0 = 0.31$ mm and $\alpha = 0.9^\circ$ from Fig. 1. (c) The data from Gabbard *et al.* [18] (orange) follow Eq. (4), consistent with conversion of surface energy into predominantly translational motion. My data (blue) deviate, indicating that a significant fraction of the energy is instead partitioned into surface oscillations and rotation after exiting the wedge.

A drop confined in a wedge experiences a capillary pressure gradient along its length. Such gradients are known to drive the self-propulsion of drops in wedges, with the direction of motion determined by wettability [12]. The same principle can be utilized to provide additional forcing to a pendant drop, provided contact-line pinning effects are negligible. This is indeed the case for water drops on superhydrophobic surfaces.

Consider a pendant drop in a wedge, with the z axis originating at the tip of the capillary [see Fig. 1(a)]. The distance between the plates then follows $h(z) = h_0 + \alpha z$, where α has units of radians. While gravity and capillary forces are balanced, the drop remains attached to the capillary tube at $z_1 = 0$, and the base of the drop is at $z_2 \approx 2\sqrt{\Omega/\pi h_0}$ for $\alpha \ll 1$. The pressure difference across a nonwetting drop can be written as $\Delta p \sim -\gamma(\frac{2}{h_0+\alpha z_2} - \frac{2}{h_0}) = \frac{2\gamma\alpha z_2}{h_0(h_0+\alpha z_2)}$. In the limit $\alpha \ll 1$, this reduces to $\Delta p \sim \alpha\gamma z_2/h_0^2$. At the point of detachment, the drop radius is of order z_2, so the mean cross-sectional area of the squeezed drop scales as $h_0 z_2$. The additional capillary force induced by the wedge thus scales as $\Delta p h_0 z_2 \approx \frac{8\alpha\gamma}{h_0}\frac{z_2^2}{4} = \frac{8\alpha\gamma}{h_0}\frac{\Omega}{\pi h_0}$, which, after absorbing numerical coefficients into a scaling prefactor c, reduces to $c\alpha\gamma\Omega/h_0^2$. The force balance on the drop can therefore be written as $\rho g\Omega + c\alpha\gamma\Omega/h_0^2 = 2\pi a\gamma$, which yields

$$\frac{\Omega_0}{\Omega} = 1 + c\alpha\left(\frac{\ell_c}{h_0}\right)^2. \tag{2}$$

Equation (2) allows for the collapse of the experimental data for a range of tip radii a, wedge angles α, and spacing between the plates h_0, as evident in Fig. 1(c). The ratio ℓ_c/h_0 provides the dominant control over drop-size reduction and is bounded above by $\ell_c/2a$.

In the limit of vanishing gravity, relevant to microgravity environments and microfluidic systems, capillarity alone governs drop detachment. In this case, Eq. (2) reduces to

$$\frac{\Omega_0}{\Omega} = c\alpha\left(\frac{\ell_c}{h_0}\right)^2,$$

highlighting that confinement alone can drive detachment even in the absence of gravitational forcing. Indeed, Dangla *et al.* [13] demonstrated capillary-driven droplet detachment in confined microfluidic geometries. In what follows, I return to the gravity-dominated regime relevant to my experiments.

While confinement enables drops smaller than the Tate limit, it is also instructive to note a complementary route for generating larger drops. One recovers Tate's law from Eq. (2) by taking $\alpha = 0$. Interestingly, Eq. (2) also suggests that one can get drops above the natural volume Ω_0 by flipping the sign of α, which corresponds to flipping the direction of the wedge. In practice, a more accessible approach is described below.

For completeness, I note that by resting a drop on a superhydrophobic surface under an incline, surface-tension pull supports only a fraction of the drop's weight [see Fig. 2(a)]. One can readily obtain drops significantly above the capillary lengthscale by simply tuning the tilt angle ϕ, as demonstrated experimentally in Fig. 2(b). The volume of the resulting drop then follows

$$\frac{\Omega_0}{\Omega} = \sin\phi, \tag{3}$$

which is plotted against the experimental data in Fig. 2(b). As ϕ goes from 0 to $\pi/2$, the system goes from sessile-drop to pendant-drop configuration. As $\phi \to \pi/2$, the detachment becomes increasingly sensitive to the distance between the nozzle and the plate. Equation (3) assumes that the surface-tension force acts parallel to the plate, which holds when the nozzle is located at approximately the same height as the drop's center of mass. Deviations from this condition lead to departures from the predicted scaling, accounting for the larger discrepancies observed as $\sin(\phi) \to 1$.

As the pendant water drop detaches from the capillary tube tip [Fig. 1(a)], the pinch-off event triggers the onset of a traveling wave along the surface of the drop. In a conventional pendant-drop setting, this traveling wave is symmetric along the z axis (see Video 1 [10]). This symmetry can be broken by holding the tube against one of the superhydrophobic walls (see Video 2 [10]). This produces a well-controlled asymmetric perturbation to the drop surface, which can be used to probe traveling wave solutions on a drop.

A more pronounced symmetry breaking occurs when the drop is squeezed between two closely spaced plates under asymmetric confinement (see Video 3 [10]). Upon exiting the wedge, the drop rapidly relaxes from an oblate ellipsoid toward a spherical shape. In the limit of negligible viscous dissipation, a substantial fraction of the associated reduction in surface energy is converted into kinetic energy [14,15]. Consistent with this mechanism, I observe that drops acquire horizontal velocity u upon exit, with smaller plate spacing leading to higher horizontal speeds [Figs. 3(a) and 3(b)]. This surface-tension-driven energy conversion underlies a range of phenomena, including spore ejection [15], colloidal catapults [16], and antifogging on nanotextured surfaces [14].

A useful point of comparison for the horizontal velocity acquired by the drop is the work of Richard and Quéré [17], Gabbard *et al.* [18] on deformation of a drop upon impact against a solid surface. In their experiments, the drop's kinetic energy is converted into surface energy as it deforms from a sphere into an oblate ellipsoid, reaching a maximum lateral extent R_m when its center of mass is lowest. The associated increase in surface area is $\frac{32\pi}{5}\gamma(R_m - R)^2$, yielding the velocity-deformation relation

$$We = \frac{48}{5}\left(\frac{R_m}{R} - 1\right)^2, \tag{4}$$

assuming all of the kinetic energy goes towards deforming the drop, where $We = \frac{\rho u^2 R}{\gamma}$ [17,18].

In contrast, in my experiments, I go from a squeezed drop to an oscillating one, and only a fraction of the released surface energy is converted into translational motion. A significant portion is instead diverted into surface waves and rotational motion (see Video 3 [10]). Consequently, the measured velocities do not follow the quadratic scaling expected from Eq. (4), as evident from Fig. 3(c). A detailed partition between translational motion and the rest, however, is nontrivial and can be a future subject of detailed numerical studies.

Overall, I show that one can easily tune the size of the detaching pendant drop without changing the capillary-tube diameter, by introducing superhydrophobic geometric confinement. The wedge confinement elicits a capillary push on the drop, directed away from the tube, thereby reducing the detachment volume below its natural value, a mechanism captured by Eq. (2).

While this relation applies to a wedge formed by two flat plates, the underlying principle can be easily extended to more effective geometric confinement. For example, the capillary push can be enhanced by replacing the wedge with a conical geometry, or by tuning the curvature of the confining walls to amplify the pressure gradient along the z axis. This technique is not limited to liquid drops in air: the same scaling arguments apply to the generation of air bubbles in a liquid, where confinement can similarly assist in producing smaller bubbles. The same scaling extends naturally to liquid-liquid interfaces, where replacing γ with the interfacial tension between immiscible fluids leads to analogous control of drop detachment. Geometric confinement thus provides a simple, robust, and extensible route for controlling drop and bubble detachment across capillary systems.

The author thanks Amir Pahlavan, Madhu Venkadesan, Larry Wilen, Johnathan Hoggarth, Zahra Shamsi, and Shomeek Mukhopadhyay for many insightful discussions. The author acknowledges support from startup funds provided by Yale University.

Data availbility. The data that support the findings of this article are not publicly available. The data are available from the authors upon reasonable request.

[1] D. Lohse, Fundamental fluid dynamics challenges in inkjet printing, Annu. Rev. Fluid Mech. **54**, 349 (2022).
[2] S. L. Anna, N. Bontoux, and H. A. Stone, Formation of dispersions using "flow focusing" in microchannels, Appl. Phys. Lett. **82**, 364 (2003).
[3] P. Garstecki, M. J. Fuerstman, H. A. Stone, and G. M. Whitesides, Formation of droplets and bubbles in a microfluidic T-junction—scaling and mechanism of break-up, Lab. Chip **6**, 437 (2006).
[4] T. Tate, On the magnitude of a drop of liquid formed under different circumstances, London, Edinburgh, Dublin Philos. Mag. J. Sci. **27**, 176 (1864).
[5] W. Fritz, Maximum volume of vapor bubbles, Physik. Zeitschr. **36**, 379 (1935).
[6] R. Kumar and N. K. Kuloor, The formation of bubbles and drops. Adv. Chem. Eng. **8**, 255 (1970).
[7] H. N. Oguz and A. Prosperetti, Dynamics of bubble growth and detachment from a needle, J. Fluid Mech. **257**, 111 (1993).
[8] H. Liu, Z. Wang, L. Gao, Y. Huang, H. Tang, X. Zhao, and W. Deng, Optofluidic resonance of a transparent liquid jet excited by a continuous wave laser, Phys. Rev. Lett. **127**, 244502 (2021).
[9] J. Fernández De La Mora, The fluid dynamics of Taylor cones, Annu. Rev. Fluid Mech. **39**, 217 (2007).
[10] See Supplemental Material at http://link.aps.org/supplemental/10.1103/95pk-yfpr for additional experimental details.
[11] R. Gupta, V. Vaikuntanathan, and D. Sivakumar, Superhydrophobic qualities of an aluminum surface coated with hydrophobic solution NeverWet, Colloids Surf., A **500**, 45 (2016).
[12] E. Reyssat, Drops and bubbles in wedges, J. Fluid Mech. **748**, 641 (2014).
[13] R. Dangla, S. C. Kayi, and C. N. Baroud, Droplet microfluidics driven by gradients of confinement, Proc. Natl. Acad. Sci. **110**, 853 (2013).
[14] T. Mouterde, G. Lehoucq, S. Xavier, A. Checco, C. T. Black, A. Rahman, T. Midavaine, C. Clanet, and D. Quéré, Antifogging abilities of model nanotextures, Nat. Mater. **16**, 658 (2017).
[15] X. Noblin, S. Yang, and J. Dumais, Surface tension propulsion of fungal spores, J. Exp. Biol. **212**, 2835 (2009).
[16] R. L. Chavez, F. Liu, J. J. Feng, and C.-H. Chen, Capillary-inertial colloidal catapults upon drop coalescence, Appl. Phys. Lett. **109**, 011601 (2016).
[17] D. Richard and D. Quéré, Bouncing water drops, Europhys. Lett. **50**, 769 (2000).
[18] C. T. Gabbard, E. A. Agüero, R. Cimpeanu, K. Kuehr, E. Silver, J.-W. Barotta, C. A. Galeano-Rios, and D. M. Harris, Drop rebound at low Weber number, J. Fluid Mech. **1019**, A25 (2025).